Porphyrin–naphthodiimide interactions as a structural motif in foldamers and supramolecular assemblies†

Zulkifli Merican, Ken D. Johnstone and Maxwell J. Gunter*

Received 14th March 2008, Accepted 16th April 2008
First published as an Advance Article on the web 16th May 2008
DOI: 10.1039/b804267e

π–π Stacking interactions between electron deficient naphthalenediimides (NDI) and electron-rich porphyrins (POR) leading to charge transfer are shown to be prevalent in linked NDI–POR and POR–NDI–POR structures. For flexibly-linked systems, intramolecular interactions lead to S-shaped foldamers in solution, whereas intermolecular association is predominant in more rigid systems. The foldamer structures can be interrupted by competing aromatic solvents, by six-coordination of metallated porphyrin derivatives, by protonation of the free base porphyrin in non-metallated structures, and in facially sterically hindered porphyrins.

Introduction

Naphthalene diimides and porphyrins have been used extensively both as structural and functional components in supramolecular chemistry. In particular, the electron acceptor qualities and the aromatic nature of *N*,*N*'-disubstituted 1,4,5,8-naphthalenediimides (NDI)[1] make them ideal candidates for use as building blocks where face-to-face charge transfer stabilisation with a suitable electron-rich aromatic donor component results in structurally defined assemblies, which can in turn be used in the templated construction of supramolecular systems. These include rotaxanes and catenanes,[2–4] including neutral, bi-stable redox- and cation-driven rotaxanes[5] and cation-templated pseudorotaxanes.[6,7] Self-stacking of the planar aromatic NDI molecules has also been the major factor in self-assembled helical nanotubes.[8] The reversible nature of the intermolecular forces involved in the stacking motif has also been used to advantage in a combinatorial approach to supramolecular assembly.[9]

A study of intermolecular stacking of porphyrins has a long history, and porphyrin self-aggregation has become a well recognised phenomenon in both aqueous and organic solvents.[10]

The combination of porphyrins with naphthodiimides and other related diimides (including smaller pyromellitimides and larger perylenediimides) has produced a wide variety of supramolecules in both covalently[11] and non-covalently[12] linked systems. The donor–acceptor nature of the resulting arrays has been utilised to considerable effect in the production of dynamic[13–16] and controllable[17] systems, both in solution and immobilised on polymer supports.[18]

The π-stacking characteristics of NDI have been utilised to advantage in the study of non-natural foldamers and aedamers. These are of particular current interest because of their applicability in emulating the dynamic structural characteristics of natural polymer systems such as proteins and DNA.[19] Although many foldamers are based on well-defined relatively rigid systems,[20] flexible examples are less common.[21] The NDI–DAN (DiAlkoxy-Naphthalene) motif has been the subject of a detailed study in the solution-state folding of dimers, trimers, and higher oligomers of linked naphthalenediimides and dialkoxynaphthalenes.[22] For example DAN–NDI–DAN trimers have been shown to adopt either intercalative, pleated or elongated structures, depending on their primary structure, solvent and temperature.

Previously, we have described the synthesis of porphyrin-based catenanes[14] and rotaxanes[15] whose templated assembly relied on a presumed NDI–POR interaction. Subsequently,[16] we reported the reversible, thermodynamically-controlled self-assembly of a series of rotaxanes, pseudorotaxanes and catenanes utilising both crown-ether-naphthalenediimide host–guest interactions, and metalloporphyrin–pyridyl coordination. For structures that comprise a porphyrin linked covalently by polyoxyethylene chains to a naphthalene diimide, which in turn is linked to a substituted pyridine **1a**, we specifically noted that there was clear evidence of intramolecular interactions between the porphyrin and the naphthalene diimide moieties as depicted in structure **1a**.

Amongst other evidence, the interactions between porphyrin and diimide was characterised by upfield shifts in the ^{1}H NMR spectrum of both the diimide and the inner porphyrin NH protons as a result of the mutual shielding of the aromatic rings in a face-to-face conformation. This implies an inherent and strong π–π interaction, possibly involving a charge-transfer, between the electron-poor diimide subunit and the electron-rich porphyrin.

In this paper, we investigate the generality of this POR–NDI porphyrin–diimide interaction, and explore how it can be utilised in the formation of foldamers for specific multi-functional systems that incorporate these units.

Results and discussion

Synthesis

Since the POR–NDI interaction appeared to be significant and general, we devised a series of structures that would enable a more detailed study of the phenomenon. In the first instance,

Chemistry, School of Science and Technology, University of New England, Armidale, NSW, 2351, Australia. E-mail: mgunter@une.edu.au; Fax: 612-6773-2368; Tel: 612-6773-2767

† Electronic supplementary information (ESI) available: ^{1}H NMR spectra and associated numbering schemes for major compounds discussed in the text; selected variable temperature NMR spectra; van't Hoff plot of **3** with DN38C10. See DOI: 10.1039/b804267e

the pyridine-terminated porphyrin diimide **1a** (Fig. 1), previously reported by us,[16] provided an opportunity to investigate the effects of intramolecular coordination on the stacking of the aromatic units. Subsequently, to ascertain if the pyridine unit is a factor in the stacking interaction, we synthesised a structural modification of **1a** in which the pyridine unit is replaced by a simple ester, **3** (Fig. 3). At the same time, we changed the attachment of the linking polyoxoethylene chain to an amide at the *para* position of the *meso* aromatic group of the porphyrin, **2** (Fig. 3), which effectively requires a longer span of the linker to achieve an intramolecularly stacked structure. Further, to promote the possibility of intramolecular foldamers, the ethyl esters of **2** and **3** were replaced with a second porphyrin in each case, resulting in **10** and **11** (Fig. 8). Replacement of the amide linkages of **10** with a less constrained secondary amine linker in **12** (Fig. 8) completed the bis-porphyrin series. The non-porphyrinic analogues **15** and **16** (Fig. 10) with varying π-acidity of the aromatic groups, provided a test of the prerequisite of the porphyrin unit in the stacking motif. Finally, shorter chain homologues of **3** and **11**, *viz.* **18** and **17** (Fig. 11), with diethyleneoxy linkages in place of the longer tetraethylenoxy chains, provided the possibility of more tightly constrained foldamers.

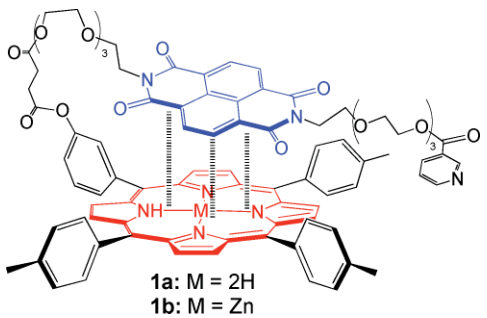

Fig. 1

The synthetic route of these derivatives was based on similar strategies used for the production of rotaxane structures previously reported by us.[15] The ethyl esters **2** and **3** (Fig 3) and their corresponding bis-porphyrin analogues **10** and **11** (Fig. 8) were produced in a single reaction by an EDC condensation of the corresponding porphyrins **14** and **13** (Fig. 8) with the bis monosuccinate ester **4** (Fig. 3) of the dihydroxy polyoxoethylene naphthodiimide **5** (Fig. 6). In each case, the presence of ethanol in the reaction mixture gave directly separable mixtures of **2** and **10**, or **3** and **11**. A similar strategy produced the shorter-chain derivatives **17** and **18** (Fig. 11). The secondary amine derived structure **12** (Fig. 8) was produced by condensation of **5** with 4-carboxybenzaldehyde, subsequent titanium tetrachloride catalysed formation of the Schiff base with the zinc derivative of porphyrin **14** and *in situ* reduction with cyanoborohydride.

Conformational studies

Pyridine-terminated diimide porphyrin 1a. Typically, the proton resonances in their ^{1}H NMR spectra of various alkyl and polyethylene glycol-substituted naphthodiimide open-chain derivatives appear around 8.7 ppm; for naphthodiimide-derived catenanes where the diimide unit is threaded through a 1,5-dinaphtho-38-crown-10 (DN38C10) macrocyclic unit, this resonance is normally shifted upfield by shielding from the crown aromatics to around 8.2–8.3 ppm.[2,7] By contrast, the diimide resonance of **1a** appears at 7.2 ppm, and shifts upfield with decreasing temperature, but is concentration-independent. This is consistent with an intramolecular folded structure as depicted in **1a**.

Zinc was inserted into the diimide-fused porphyrin producing **1b** (Fig. 1), to establish whether this might disrupt the porphyrin–diimide interaction: the terminal pyridine of **1b** was expected to coordinate intramolecularly to the zinc porphyrin and thus interrupt the porphyrin–diimide interaction. However, proton NMR analysis of the compound showed diimide upfield shifts indicative of a porphyrin–diimide interaction being maintained, in addition to the terminal pyridyl–zinc coordination. This suggests the structure shown in Fig. 2, with the long tetraethylene glycol-derived linker groups allowing both the porphyrin–diimide interaction on one face of the porphyrin and the pyridine–zinc coordination on the other.

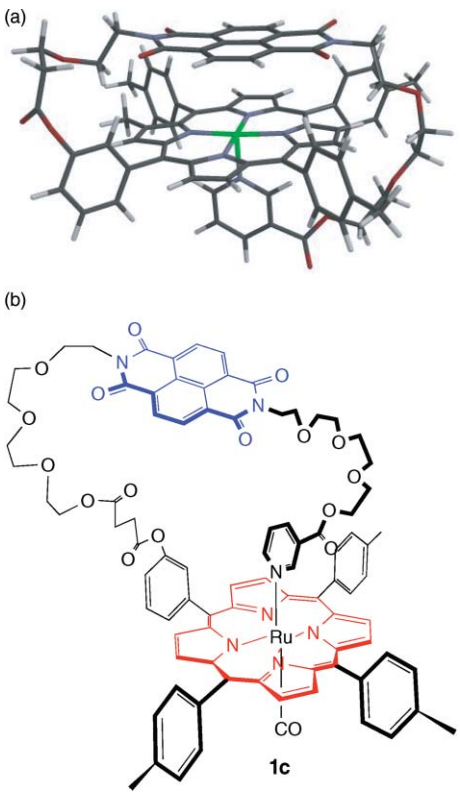

Fig. 2 Above: the folding effect expected‡ for the zinc metallated derivative **1b**, incorporating both pyridine–zinc coordination and diimide–porphyrin interaction. Two of the linker ethyleneoxy groups from each side of the diimide sub-unit have been omitted for clarity. Below: the expected conformation of **1c**, the ruthenium(II) metallated derivative of **1a**. The terminal pyridine coordinates to the central ruthenium(II) ion, while the carbonyl ligand on the alternate porphyrin face prevents diimide–porphyrin stacking interactions.

The simple modification of **1a**, by utilising a six-coordinate ruthenium(II) with its carbonyl ligand as the central porphyrin metal ion in the place of zinc, was expected to prevent such

‡ This depiction is suggested, and is not an energy minimised structure.

a folding effect, as the carbonyl would block the face of the porphyrin opposite to the pyridyl coordinating face. Proton NMR analysis of the resulting structure **1c** (Fig. 2), previously reported by us,[16] showed the diimide peak in its unshielded (δ 8.7) position, suggesting successful prevention of the porphyrin–diimide interaction and the structural conformation shown in Fig. 1.

Mono-porphyrin linked diimides. In the case of the mono-porphyrin diimide long chain units **2** and **3** (Fig. 3) with ethyl esters replacing the pyridine unit of **1a**, the NMR spectra revealed

R	R'	Compound
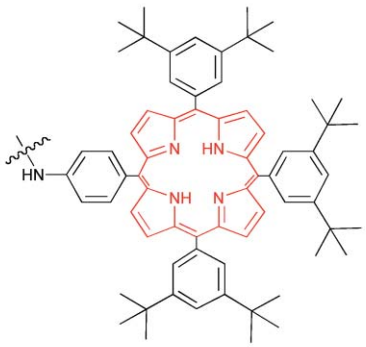	OEt	**2**
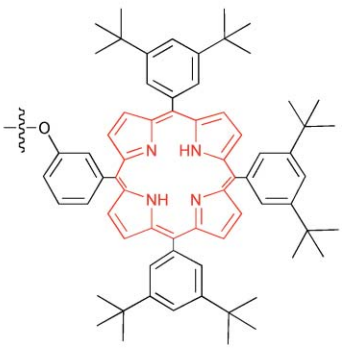	OEt	**3**
OH	OH	**4**

Fig. 3

the presence of intramolecular POR–NDI interactions similar to those seen in **1a** (ESI, Fig. S1 and S2†). In these cases, because of the molecular asymmetry, the diimide proton signals now appear as AB quartets, but at 7.76–7.88 ppm for **2** and 7.19–7.29 ppm for **3**, still significantly shielded compared to typical unassociated 'free' diimides; the porphyrin core NH protons were also still shielded at −3.38 ppm for **2** and −3.84 ppm for **3**.

Since these porphyrin mono-stoppered derivatives are capable of threading through a DN38C10 macrocycle, the formation of the resultant pseudorotaxane should be accompanied by a release of the folded structure to accommodate the macrocycle. Indeed, the spectrum of a 1 : 1 mixture of **3** and DN38C10 in deuterochloroform showed peaks for both bound and unbound species over a range of low temperatures where the system was in slow exchange (<270 K).§ In this case, the NDI proton signal was observable in both its unbound (~7.2 ppm) and bound (~8.2 ppm) positions. The bound position was identical to that for the pseudorotaxane formed from the non-porphyrinic dicarboxylic acid precursor **4** and DN38C10, and this peak grew at the expense of that for the unbound (but folded) species at 7.2 ppm. This is consistent with the formation of the pseudorotaxane structure [**DN38C10**.**3**] (Fig. 4) in which the encircling crown ether now precludes the foldamer conformation, as expected.

From this data, the binding strength of the DN38C10 complex with **3** was calculated to be 3.98×10^2 M^{-1} at 243 K. This compares to the K_a of the complex between **4** and DN38C10 at the same temperature of 3.52×10^3 M^{-1}, and indicates that while DN38C10 binds to **3** less strongly, it adopts a similar open conformation when bound. A van't Hoff plot of this system gave a non-linear relationship between $R \ln K$ and $1/T$ (see ESI, Fig. S3†), as did the [**DN38C10**.**1a**] system, which is indicative of a conformational or other change accompanying the binding process (*i.e.* in these cases, an unravelling of the foldamer).¶

§ At higher temperatures, in the fast exchange regime, only a temperature-dependent time-averaged peak is seen for the diimide resonance.

¶ The reason for the weaker complexation is unclear, as intuitively one might expect a stronger interaction with the porphyrin-stoppered adduct, as this has the possibility of an alternative site for a π-stacked complex, now between the DN38C10 aromatics and the porphyrin ring. We had previously reported[15] a non-linear van't Hoff plot for the system involving DN38C10 and **1c** in the formation of a pseudo-catenane, with a K_a of 140 M^{-1} at 273 K, and a non-zero heat capacity term ΔC_p as a result of an unfolding required for the formation of the pseudo-catenane. This is similar to the results seen for the free base derivative **1a**.

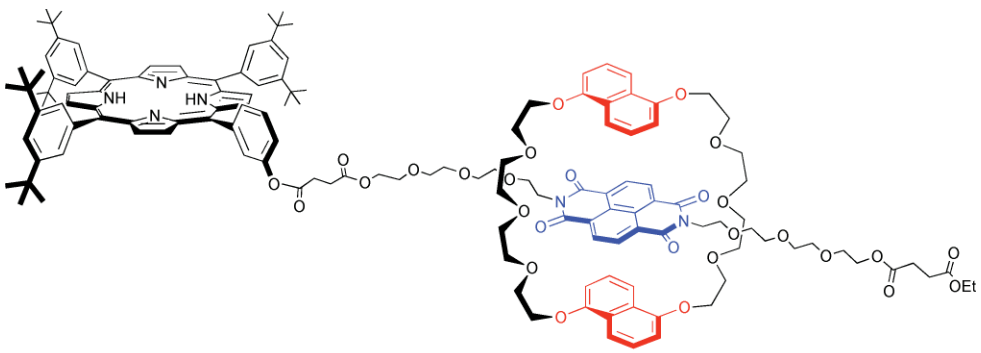

[DN38C10.3]

Fig. 4

The porphyrin–diimide orientation in these systems is expected to be similar to the calculated structure shown in Fig. 5, with the diimide lying face-to-face with the porphyrin to optimise the π–π interactions between the two aromatics. The space-filling model also shown in Fig. 5 illustrates that the diimide appears to have an ideal size and shape to match the cavity afforded by the *meso*-aromatics on the porphyrin face. It is likely that it is a combination of the π–π interactions and the snug fitting nature of the POR–NDI porphyrin–diimide interaction that makes it so significant, and if so, then it is expected that relatively stable complexes should be maintained intermolecularly for un-linked porphyrins and diimides.

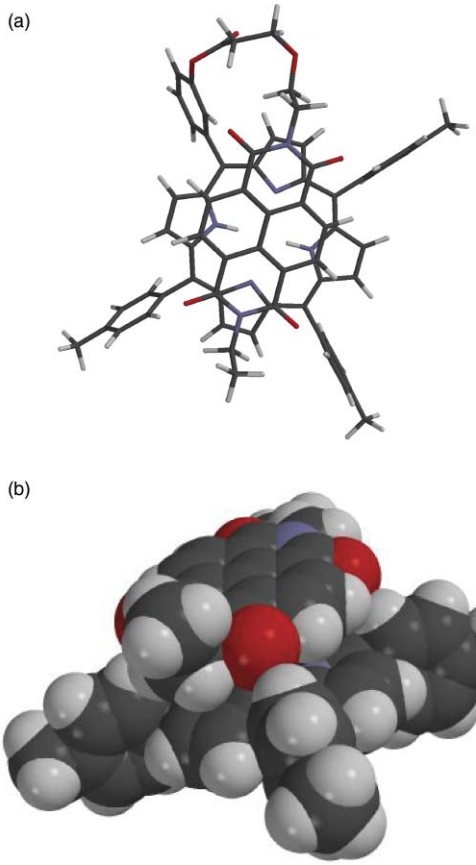

Fig. 5 Depiction of the calculated* diimide–porphyrin interaction in **1a**: top view, with the diimide lying above the porphyrin face (top); and space-filling depiction (bottom). Two of the linker ethyleneoxy groups were omitted from the linked side of the diimide sub-unit and only an ethyl group was included on the other (free) side of the diimide to simplify the calculation.

Intermolecular systems. This was validated by the fact that an equimolar mixture of tetratolyl porphyrin **6** with naphthalene diimide **5**[4] (Fig. 6) in $CDCl_3$ produced diimide and porphyrin N–H proton NMR upfield shifts similar to **1a**, indicating an intermolecular interaction. The association constant for **5** with **6** was calculated as $15.6 \pm 1.2\ M^{-1}$ from NMR titration experiments.

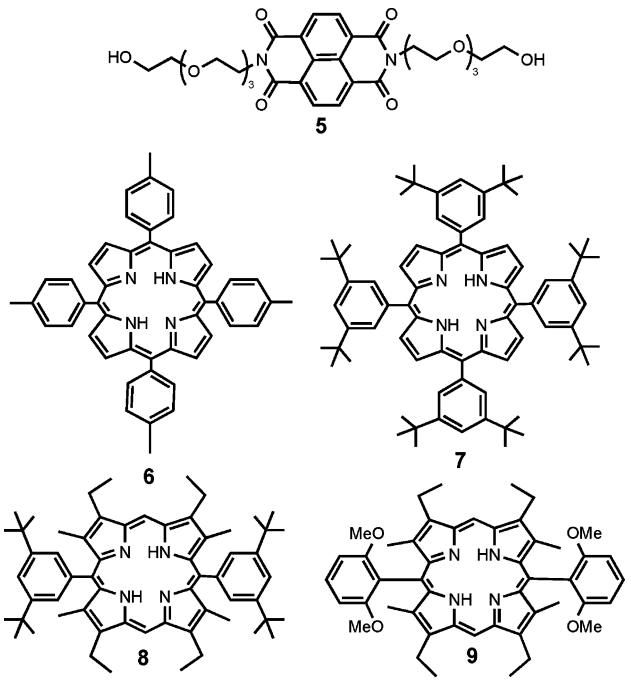

Fig. 6

It is expected that a conformation as depicted in Fig. 5 would be destabilised by any porphyrin with sterically demanding groups on each of its faces. Thus, a series of porphyrins, including **6**, **7**, **8** and **9** (Fig. 6) were analysed using NMR methods. **9**, with its bulky methoxy *ortho* substituents, was specifically designed to block any close approach of the diimide and porphyrin. The other porphyrins contained either two or four *meso*- aromatics with *para* or *meta* substituents.

When individually mixed with **5** in $CDCl_3$, **6**, **7** and **8** each exhibited significant diimide shifts, indicative of the expected diimide–porphyrin interaction. However, the bulky methoxy *ortho* substituted porphyrin **9** showed only an unshielded diimide peak at δ 8.7, suggesting a blocking of the diimide–porphyrin interaction through steric hindrance. These results were duplicated using a pyromellitimide thread in place of the naphthalene diimide, with the same series of porphyrins.

UV analysis confirmed this result: difference absorption spectra were measured between the porphyrin–diimide systems and equimolar solutions of the respective porphyrin (Fig. 7). Since the diimide **5** exhibits no absorption above 400 nm, any peaks observed must arise from new absorbances caused by the interaction between the diimide and porphyrin, specifically charge-transfer bands. The mixtures of **5** with **6**, and **5** with **7** exhibited a new band that can be attributed to a charge transfer absorption at 432 nm, while the corresponding band for the mixture of **5** with **8** appeared at 426 nm. The sterically-hindered porphyrin **9** showed no charge transfer absorbance in the examined spectral region. These results are consistent with the corresponding NMR findings that **9**, with its sterically-hindering *ortho* substitution, is prevented from forming a stable complex. Similar charge-transfer absorption results were found using pyromellitimide in place of the naphthalene diimide thread.

* AM1 semiempirical energy minimisation calculation performed using the MacSPARTAN program. The porphyrin with its meso-substituted aromatics was minimised separately first, then this component of the structure was locked, while the diimide thread component was allowed to move. The resultant structure shown is the calculated lowest energy position for the diimide.

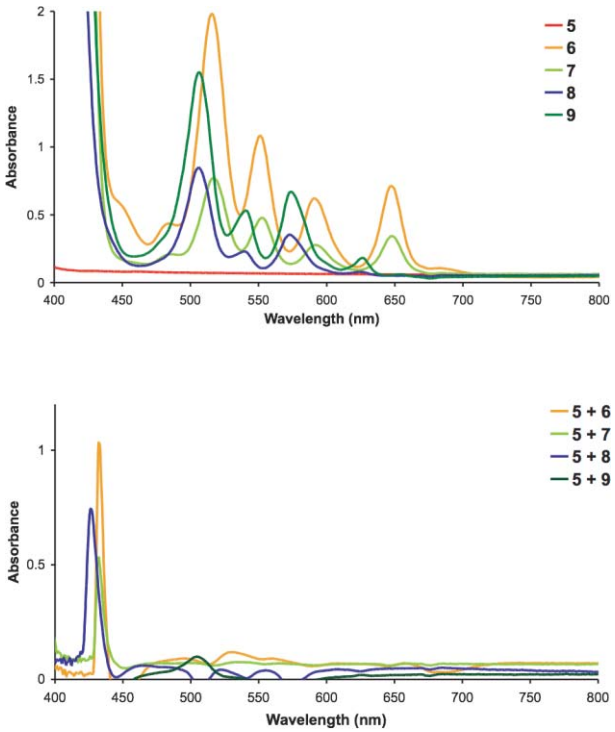

Fig. 7 UV–vis spectra in $CHCl_3$ of: **5**, **6**, **7**, **8** and **9** (top); and difference spectra of equimolar mixtures of **5** with: **6**, **7**, **8** and **9** (bottom), measured against the respective porphyrin component.

Bis-linked porphyrin diimide foldamers. This inherent capacity for face-to-face π-stacking between facially unhindered *meso*-substituted porphyrins and naphthodiimides is also evident in other linked systems which can adopt folded conformations in solution, similar to that seen in **1**, **2**, and **3**.

This can be seen for example in ^{1}H NMR spectra of the three bis-porphyrin adducts **10**, **11** and **12** (Fig. 8), all of which showed significant upfield shifts of the diimide proton resonances (7.42, 6.93 and 7.11 ppm in $CDCl_3$ for **10**, **11** and **12**, respectively), indicative of a solution conformation involving a shielding of the diimide unit, either by an inter- or intra-molecular interaction; an S-shaped foldamer POR–NDI–POR as depicted in Fig. 8 is suggested (see ESI, Fig. S4, S5, S6†).

Complementary shifts of the inner NH protons of the porphyrin ($\Delta\delta$ −0.50, −0.68 and −0.59 ppm respectively in each case, compared to the unattached porphyrin precursors **13** or **14**) are consistent with such a foldamer conformation with face-to-face stacking of the diimide and porphyrin units. The folding of the polyoxyethylene chains inherent in the S-shaped foldamer was also apparent by NOESY correlations between the protons adjacent to the diimide N, and the succinyl ester group protons in **11**.

Concentration-invariance of the spectrum is consistent with a foldamer, rather than possible alternative intermolecular stacking. At higher temperatures, the diimide and inner porphyrin NH resonances gradually shift downfield in tandem, as π–π stacking is diminished ($\Delta\delta$ +0.28 between 303 K and 328 K for **10** in $CDCl_3$); there is minimal change in other resonances (see ESI, Fig. S7†). Similar temperature dependence was observed for the ester-linked **11** and the amine-linked **12**.

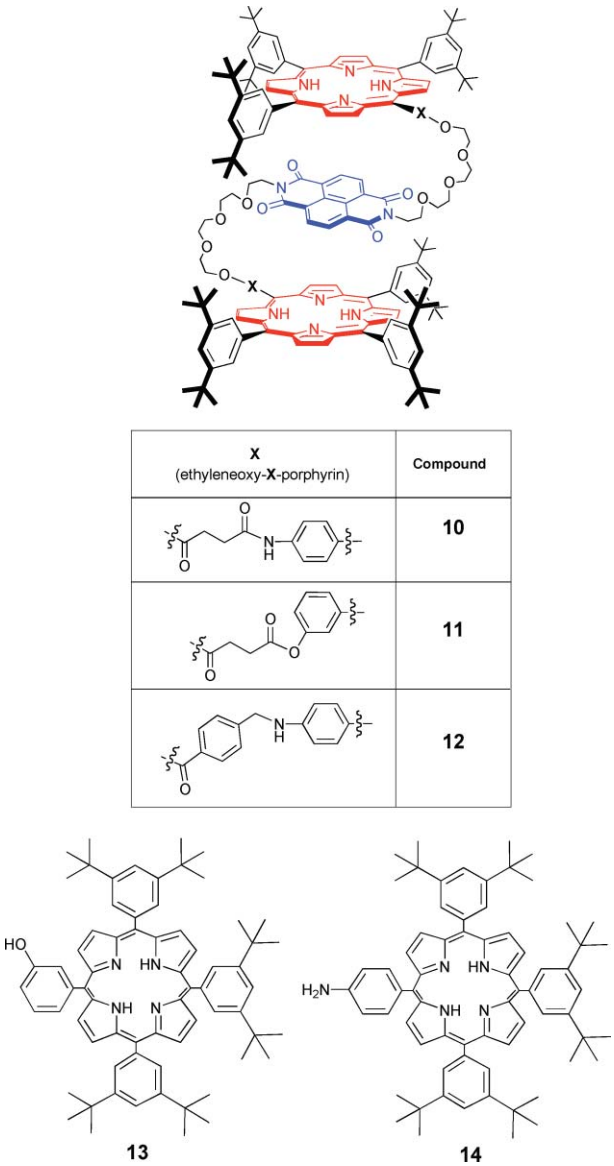

Fig. 8

For the *meta*-linked derivative **11**, the mutual shielding of the porphyrin and diimide units is even more pronounced than in the *para*-substituted amide analogue **10**. The diimide protons of **11** are upfield shifted by −1.80 ppm, compared to −1.31 ppm for **10**, and the porphyrin NH's are also more shielded ($\Delta\delta$ −0.68 ppm compared to −0.50 ppm). In this case, because of the absence of the plane of symmetry through the porphyrin unit, the *ortho*-protons of the 3,5-di-*tert*-butyl groups on the *meso*-substituents appeared as closely coupled separated resonances. Significantly, only one of these resonances showed ROESY correlations with the diimide protons, obviously the *ortho*-protons on the face of the porphyrin proximal to the diimide in the foldamer structure.

Further evidence for the S-shaped foldamer conformation was derived from metallation of the porphyrin. Thus, in the corresponding zinc derivative of **10** it was confirmed that there was little effect on the diimide–porphyrin interaction in the non-coordinating $CDCl_3$ solvent. Indeed, the diimide resonance

now appeared at even higher field (δ 7.19 ppm), indicating an enhanced interaction. This may be purely electronic in origin (less electronegative zinc derivative compared to free base), or perhaps due to an augmentation by appropriate coordination of the zinc ion to one of the O atoms in the polyether chain. Shifts in many of the polyether methylene resonances favour the latter. Nevertheless, since zinc porphyrins readily form 5-coordinate complexes in the presence of nitrogenous bases, the addition of pyridine may cause unfolding of the bis-adduct by displacing the diimide; on the other hand, axial coordination at the "outside" faces of the zinc porphyrins would have little effect on the diimide–porphyrin stacking, as depicted in Fig. 9B.

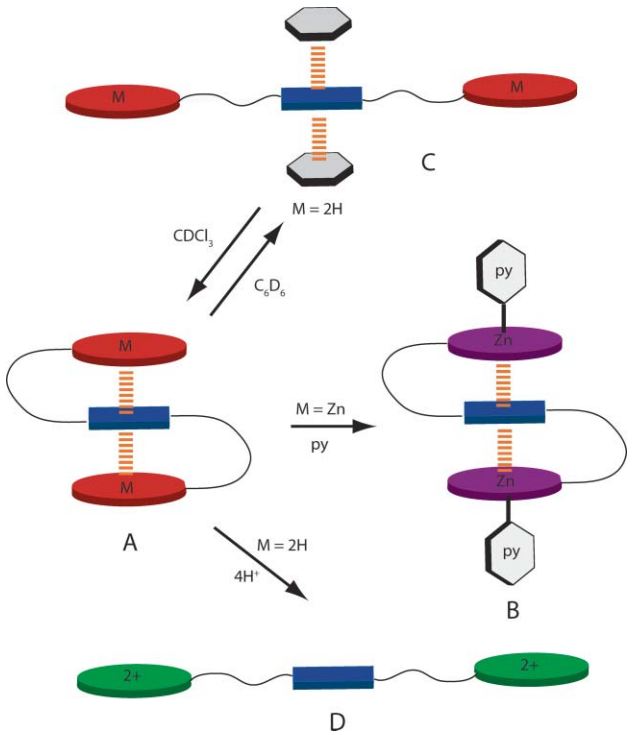

Fig. 9 Depiction of the folded and extended conformations in the bis-porphyrin diimide derivatives **10**, **11**, and **12** as deduced from NMR measurements. The dashed lines indicate co-facial π–π interactions.

Thus, on increasing addition of pyridine to a $CDCl_3$ solution of **Zn10**, as well as small expected shifts in some of the porphyrin resonances, broadened zinc-coordinated pyridine resonances appeared, in a pattern and position typical of pyridine-coordinated zinc porphyrins (for these complexes, ligand exchange is fast on the NMR chemical shift timescale, so the ligand resonances are broadened and shifted upfield and gradually move downfield with increasing pyridine addition). After two mole equivalents of pyridine per zinc porphyrin, the diimide resonance had moved slightly downfield to a limiting position of 7.45 ppm, still well short of the value of 8.7 ppm expected for a non-interacting, unfolded conformation. At the same time, the previously shifted polyether methylene signals now moved back to their approximate position as in **10**, consistent with a replacement of the presumed polyether oxygen coordination to the zinc by the stronger pyridine ligand (see ESI, Fig. S8†). This is then compatible with a structure with "outside" coordination of the pyridine, as indicated in Fig. 9B.

Further evidence for the POR–NDI–POR foldamer structure resulting from π–π interactions was provided by the ^{1}H NMR spectrum of **10** in benzene-d_6. In this solvent, the pyrrolic NH protons were now shifted downfield to −2.74 ppm ($\Delta\delta$ +0.45 ppm relative to the spectrum in $CDCl_3$) (see ESI, Fig. S9†). This is a similar chemical shift to that for the previously reported[15] [2]rotaxane comprising **10** threaded through the dinaphtho-38-crown-10 macrocycle, [**DN38C10**.**10**]. In this rotaxane, the NDI unit is sandwiched between the aromatic groups of the crown ether, which effectively prevents any POR–NDI interactions. By analogy then, in this case, this is consistent with an unfolded conformation with the POR–NDI interactions replaced by benzene–NDI π–π stacking, as indicated in Fig. 9C.

The benzene–diimide interactions in this solvent also impose an enhanced upfield shift on the naphthodiimide protons, which now appear at 6.85 ppm. The fact that these protons are shifted further upfield than in $CDCl_3$ can be rationalised by (i) a more effective overlap of the smaller benzene π-system compared to larger, more diffuse, and peripherally crowded porphyrin rings; and (ii) an equilibrium effect shifted towards more complete intermolecular complexation as a result of the larger effective molarity of the π-donor constituent in the neat d_6-benzene solvent.

Although zinc insertion into the porphyrin did not interfere with the S-shaped POR–NDI–POR foldamer conformation, protonation of the free base porphyrin was effective in destroying the stabilising interactions, leading to unfolding. This was clearly seen by the downfield shift of the diimide proton signal in the NMR spectrum of **10** in $CDCl_3$ containing trifluoroacetic acid, to 8.72 ppm, a chemical shift typical of 'free' naphthodiimides in the absence of inter- or intra-molecular π-stacking effects (see ESI, Fig. S10†). Protonation of free base porphyrins is accompanied by a ruffling of the planar structure,[23] which apparently in this case is sufficient to introduce steric constraints to any stacked conformations of the porphyrin and diimide aromatic systems. In this instance, the NH protons in the porphyrin core were no longer diagnostic, as they appeared upfield shifted as expected for a protonated porphyrin, as were the β-pyrrolic and other porphyrinic aromatic resonances.

The π-stacking interactions responsible for the foldamer structure in the POR–NDI–POR systems are not maintained if the porphyrin units are replaced by smaller aromatic groups. The non-porphyrinic analogues **15** and **16** (Fig. 10) where the porphyrin has

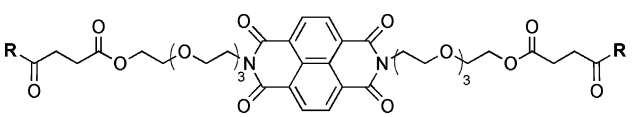

R	Compound
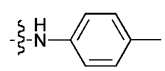	**15**
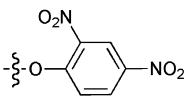	**16**

Fig. 10

been replaced by either *p*-tolyl or 2,4-dinitrophenyl groups show no evidence of shielding of the naphthodiimide proton signals in solution, and they appear in the 'normal' range, *viz*. 8.67 and 8.72 ppm, respectively, indicative of an extended, unfolded conformation.

The folded conformation is also maintained with the shorter dioxyethylene linked derivatives **17** and **18** (Fig. 11), as evidenced by: the upfield shifts of both diimide ($\Delta\delta$ −2.09 and −1.88 ppm respectively) and porphyrin NH ($\Delta\delta$ −0.79 and −1.41 ppm, respectively) resonances in their NMR spectra; a NOESY correlation between the diimide and the downfield shifted (deshielded by the diimide) *ortho*$_1$ protons of the *meso* aromatic groups, as well as the β-pyrrolic protons; and an enhanced deshielding (compared to the longer chain derivative **11**) of the methylene signals in the dioxyethylene chains as a result of stronger deshielding by the diimide and porphyrin rings in this more tightly folded structure.

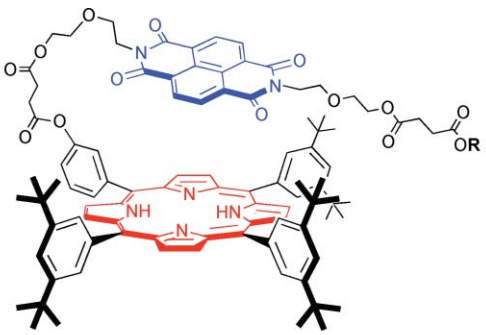

R	Compound
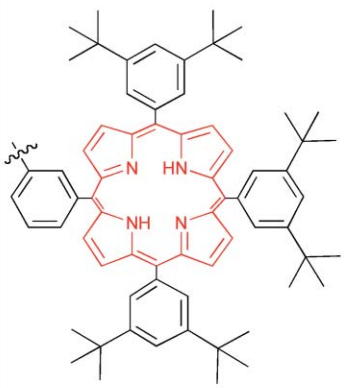	**17**
Et	**18**

Fig. 11

On the other hand, it is obvious that the more rigidly constrained bis-porphyrin diimide **19** (Fig. 12), which has previously been incorporated as the thread component of a [2]rotaxane,[15] cannot form the S-shaped foldamer structure of the more flexible systems described above. Nevertheless, the diimide resonances of this molecule appear upfield from the 'normal' range at 7.45 ppm, with the porphyrin NH's also somewhat upfield at −2.95 ppm.

However, in this case, the shifts are concentration-dependent, indicating an *inter*-molecular stacking pattern. NOESY

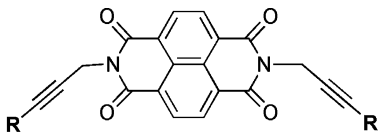

19

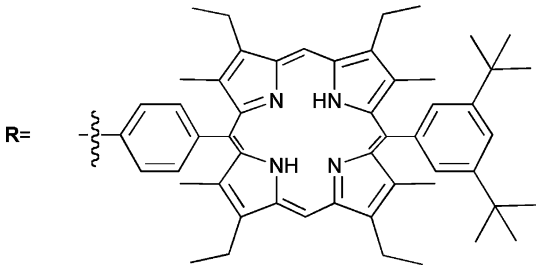

Fig. 12

correlations between the propynyl methylene and the β-methyl and ethyl resonances in more concentrated solutions are further evidence of an intermolecular stacking between diimide and porphyrin units, as the relatively constrained geometry of **19** would render intramolecular correlations unlikely. This interaction is not possible in the rotaxane consisting of **19** as the thread unit through a DN38C10 macrocycle, [**DN38C10**.**19**], as we have reported previously,[15] and the NMR shifts are as expected for these types of rotaxanes.

Experimental

In the following descriptions, NMR assignments follow the numbering schemes indicated for the respective compounds in the ESI.†

2-(2-(2-(2-(2-(5,10,15-Tris((3,5-di-*tert*-butyl)phenyl)-20-(4-(3-carboxypropionamido)phenyl)porphyrinyloxy)ethoxy)ethoxy)ethoxy)-ethyl)-7-(2-(2-(2-(2-(3-ethoxycarbonyloxy)propionyloxy)ethoxy)-ethoxy)ethoxy)ethyl)benzo[*lmn*]-(3,8)phenanthroline-1,3,6,8-tetraone 2 and 2,7-bis-(2-(2-(2-(2-(5,10,15-tris((3,5-di-*tert*-butyl)phenyl)-20-(4-(3-carboxypropionamido)phenyl)-porphyrinyloxy)ethoxy)ethoxy)ethoxy)ethyl)benzo[*lmn*]-(3,8)phenanthroline-1,3,6,8-tetraone 10

To a solution of 2,7-bis-(2-(2-(2-(2-(3-carboxypropionyloxy)ethoxy)ethoxy)ethoxy)ethyl)benzo[*lmn*]-(3,8)phenanthroline-1,3,6,8-tetraone **4**[15] (25 mg, 3.05×10^{-5} mol) in freshly distilled $CHCl_3$ (14 mL) containing EtOH (15 μl) were sequentially added EDC (14.6 mg, 7.63×10^{-5} mol), 1-hydroxybenzotriazole, HOBT (16.5 mg, 1.22×10^{-4} mol) and 5,10,15-tris((3,5-di-*tert*-butyl)phenyl)-20-(4-aminophenyl)porphyrin[24] (62 mg, 6.41×10^{-5} mol). Dry Et_3N (14 μl, 1.01×10^{-4} mol) was then added and the reaction was stirred for 7 d (N_2, dark). Excess solvent was removed *in vacuo*, and the crude mixture was washed with dilute HCl (2 M), water, saturated $NaHCO_3$, water (3×) and taken up in DCM. The organic layer was then dried (Na_2SO_4) and evaporated *in vacuo*. Purification was carried out using preparative TLC silica plates with 5% MeOH–DCM as the eluant to afford unreacted starting porphyrin (14 mg, 22.5% recovered),

bis-stoppered porphyrin thread **10**, and mono-stoppered thread **2**:

10 (11.8 mg, 14%) as a purple solid (from MeOH–$CHCl_3$); mp 184–187°C; *m/z* (ES-MS) ($C_{174}H_{200}N_{12}O_{16}$): $[M + 2H]^{2+}$ 1358.774 (calc. 1358.771); ^1H NMR (300 MHz, $CDCl_3$) δ 8.87 (16H, m, H2, 3, 7, 8, 12, 13, 17, 18), 8.17 (4H, d, *J* 6, H22), 8.17–8.15 (2H, hidden, H23), 8.12 (12H, ms, *ortho*), 7.90 (4H, d, *J* 9, H21), 7.79 (6H, ms, *para*), 7.42 (4H, s, ND), 4.30 (4H, t, *J* 6, H26), 4.05 (4H, t, *J* 6, H33), 3.70 (4H, t, *J* 6, H27), 3.60 (12H, m, H28–30), 3.52 (8H, m, H31–32), 2.85 (4H, d, *J* 6, H34), 2.76 (4H, d, *J* 6, H35), 1.53 (108H, s, *t-butyl*), −3.19 (4H, s, H25).

2 (2.7 mg, 5%) as a purple solid (from MeOH–$CHCl_3$); mp 100–104°C; *m/z* (ESI-MS) ($C_{108}H_{127}N_7O_{17}$): $[M + H]^+$ 1794.923 (calc. 1794.937); ^1H NMR (300 MHz, $CDCl_3$) δ 8.85–8.80 (8H, m, H2, 3, 7, 8, 12, 13, 17, 18), 8.26 (1H, br, H23), 8.20 (2H, d, *J* 9, H22), 8.14–8.12 (6H, m, *ortho*), 7.95 (2H, d, *J* 9, H21), 7.88 (2H, d, *J* 8, ND2), 7.79–7.77 (3H, m, *para*), 7.76 (2H, d, *J* 8, ND1), 4.38 (2H, t, *J* 5, H26), 4.23 (2H, t, *J* 6, H33), 4.17–4.11 (4H, m, H45, 46), 4.09 (2H, t, *J* 7, H38), 3.78 (2H, t, *J* 5, H27), 3.70–3.64 (10H, m, H28–32), 3.59–3.49 (12H, m, H39–44), 2.89 (2H, t, *J* 6, H34), 2.85 (2H, t, *J* 6, H35), 2.58–2.56 (4H, m, H36, 37), 1.54 (54H, s, *t-butyl*), 1.23 (3H, t, *J* 6, H47), −3.38 (2H, s, H25).

2-(2-(2-(2-(2-(5,10,15-Tris((3,5-di-*tert*-butyl)phenyl)-20-(3-(3-carboxypropionoyl)phenyl)porphyrinyloxy)ethoxy)ethoxy)ethoxy)-ethyl)-7-(2-(2-(2-(2-(3-ethoxycarbonyloxy)propionyloxy)ethoxy)-ethoxy)ethoxy)ethyl)benzo[*lmn*]-(3,8)phenanthroline-1,3,6,8-tetraone 3 and 2,7-bis-(2-(2-(2-(2-(5,10,15-tris((3,5-di-*tert*-butyl)phenyl)-20-(3-(3-carboxypropionoyl)phenyl)porphyrinyloxy)-ethoxy)ethoxy)ethoxy)ethyl)benzo[*lmn*]-(3,8)phenanthroline-1,3,6,8-tetraone 11

This was synthesised by a method similar to that described above for **2**, using 2,7-bis-(2-(2-(2-(2-(3-carboxypropionyloxy)ethoxy)ethoxy)ethoxy)ethyl)benzo[*lmn*]-(3,8)phenanthroline-1,3,6,8-tetraone (23 mg, 2.81×10^{-5} mol), dry $CHCl_3$ (13 mL), EtOH (15 µl) dry Et_3N (13 µl), EDC (13.5 mg, 7.04×10^{-5} mol), HOBT (7.6 mg, 5.62×10^{-5} mol) and 5,10,15-*tris*((3,5-di-*tert*-butyl)phenyl)-20-(3-hydroxyphenyl)porphyrin[15] (60 mg, 6.20×10^{-5} mol). The crude product was purified by silica column chromatography (1% MeOH–$CHCl_3$) to give unreacted porphyrin (10.5 mg, 17.5%), the bis-porphyrin thread unit **11** and **3**:

11 as a purple solid (from MeOH–$CHCl_3$) (17.2 mg, 23%); mp 182–184 °C; *m/z* (ESI-MS) ($C_{174}H_{198}N_{10}O_{18}$): $[M + 2H]^{2+}$ 1359.759 (calc. 1359.755); ^1H NMR (300 MHz, $CDCl_3$) δ 8.86–8.81 (16H, m, H2, 3, 7, 8, 12, 13, 17, 18), 8.34 (6H, s, *ortho*$_1$), 8.23 (2H, d, *J* 3, H21), 7.94 (2H, d, *J* 6, H22), 7.92 (6H, s, *ortho*$_2$), 7.80 (6H, s, *para*), 7.67 (2H, t, *J* 6, H23), 7.52 (2H, d, *J* 6, H24), 6.93 (4H, s, ND), 4.22 (4H, t, *J* 6, H26), 4.00 (4H, t, *J* 6, H33), 3.61 (4H, t, *J* 6, H27), 3.48 (12H, m, H28–30), 3.43 (8H, m, H31–32), 3.01 (4H, t, *J* 6, H35), 2.84 (4H, t, *J* 6, H34), 1.60 (54H, s, *t-butyl*$_1$), 1.48 (54H, s, *t-butyl*$_2$), −3.40 (4H, s, H25).

3 (3.3 mg, 6.6%) as a purple solid (from MeOH–$CHCl_3$); mp 95–99 °C; *m/z* (ES-MS) ($C_{108}H_{126}N_6O_{18}$): $[M + Na]^+$ 1817.904 (calc. 1817.903), $[M + H]^+$ 1795.922 (calcd. 1795.921); ^1H NMR (300 MHz, $CDCl_3$) δ 8.85–8.79 (8H, m, H2, 3, 7, 8, 12, 13, 17, 18), 8.53 (3H, s, *ortho*$_1$), 8.41 (1H, s, H21), 7.83 (1H, d, *J* 6, H22), 7.82 (3H, s, *ortho*$_2$), 7.79 (3H, s, *para*), 7.65 (1H, t, *J* 6, H23), 7.50 (1H, d, *J* 6, H24), 7.29 (2H, d, *J* 9, ND_2), 7.19 (2H, d, *J* 6, ND_1), 4.15 (2H, t, *J* 6, H26), 4.11 (2H, t, *J* 6, H33), 4.08 (4H, m, H45, 46), 4.01 (2H, t, *J* 6, H38), 3.59 (2H, t, *J* 6, H27), 3.53 (10H, m, H28–32), 3.50–3.46 (12H, m, H39–44), 3.08 (2H, t, *J* 6, H35), 2.91 (2H, t, *J* 6, H34), 2.59 (4H, t, *J* 3, H36, 37), 1.66 (27H, s, *t-butyl*$_1$), 1.46 (27H, s, *t-butyl*$_2$), 1.24 (3H, t, *J* 6, H47), −3.84 (2H, s, H25).

2,7-Bis(2-(2-(2-(2-(4-formylphenylcarboxy)-ethoxy)-ethoxy)-ethoxy)-ethyl)benzo[*lmn*]-[3,8]phenanthroline-1,3,6,8-tetraone 20

This was synthesised by an analogous method to that used for **2**, using dihydroxydiimide thread **5** (0.101 g, 1.64×10^{-4} mol), 4-carboxybenzaldehyde (0.079 g, 5.26×10^{-4} mol), dry DCM (10 mL), dry Et_3N (76 µl, 5.71×10^{-4} mol), EDC (0.160 g, 8.35×10^{-4} mol), HOBT (0.088 g, 6.51×10^{-4} mol) and stirring for 7 d. Upon removal of excess solvent, a yellow oil (144 mg, 99.5%) was obtained, which was sufficiently pure for further reaction. (ESI-MS) ($C_{46}H_{46}N_2O_{16}$): $[M + Na]^+$ 905.276 (calcd. 905.275); ^1H NMR (300 MHz, $CDCl_3$) δ 10.02 (2H, s, H48), 8.65 (4H, s, ND), 8.13 (4H, d, *J* 9, H34), 7.88 (4H, d, *J* 9, H35), 4.43–4.36 (8H, m, H26, 33), 3.80 (8H, m, H27, 28), 3.65–3.64 (4H, m, H30), 3.63–3.56 (12H, m, H29, 31, 32).

5,10,15-Tris((3,5-di-*tert*-butyl)phenyl)-20-(4-aminophenyl)porphyrinato)zinc(II) 21

Zinc was inserted into the free-base amino phenyl porphyrin using the standard method ($Zn(OAc)_2$–DCM–MeOH) to give **21** as a reddish purple solid (73 mg 98%); mp 299–302 °C; ^1H NMR (300 MHz, $CDCl_3$) δ 8.96–8.91 (6H, m, H3, 7, 8, 12, 13, 17), 8.78 (2H, d, *J* 5, H2, 18), 8.11 (2H, d, *J* 2, *ortho*), 8.06 (4H, d, *J* 2, *ortho*), 7.76 (1H, t, *J* 2, *para*), 7.72 (2H, t, *J* 2, *para*), 7.62 (2H, d, *J* 8, H21), 5.63 (2H, br, H22), 1.50 (27H, s, *t-butyl*), 1.41 (27H, s, *t-butyl*), −1.35 (1H, br, H23).

2,7-Bis(2-(2-(2-(2-(4-(5-(phen-4-yl)10,15,20-tris((3,5-di-*tert*-butyl)phenyl)porphyrinyl)-aminophenyl-4-benzylcarboxy)-ethoxy)-ethoxy)-ethoxy)-ethyl)benzo[*lmn*]-[3,8]phenanthroline-1,3,6,8-tetraone 12

Following the modified method outlined by Barney *et al*,[25] to a solution of naphthodiimide dialdehyde **20** (21.4 mg, 2.43×10^{-5} mol), dry DCM (50 mL), and dry Et_3N (10 µl, 7.17×10^{-5} mol) was added $NaBH_3CN$ (4.6 mg, 7.29×10^{-5} mol). The solution immediately went bright red, which was strongly indicative of charge transfer complex formation. The mixture was equilibrated for 60 min at RT after which time zinc amino phenyl porphyrin **21** (50 mg, 4.86×10^{-5} mol) and a solution of $TiCl_4$ in DCM (12.50 µl, 1.25×10^{-5} mol) were added. The reaction was then stirred for 18 h before it was quenched with a THF solution of $NaBH_3CN$ and the stirring was continued for a further 6 h. The reaction mixture was then washed with 5 M NaOH, water (3×) and dried (Na_2SO_4). Excess solvent was removed *in vacuo.* Multiple purifications on preparative TLC silica plates (2% MeOH–DCM) afforded the free-base derivative of amino phenyl porphyrin **21** (14 mg, 29.0% recovered), bis adduct **12** (5.8 mg, 4.3%), and the corresponding mono-porphyrin adduct (16.8 mg, 14%).

12 (from $CHCl_3$–MeOH) mp 211–215 °C; *m/z* (ES-MS) ($C_{182}H_{204}N_{12}O_{14}$): $[M + Li]^+$ 2789 (calcd. 2788.56), $[M + 2H]^{2+}$

1392.793 (calcd. 1392.792); ^{1}H NMR (300 MHz, $CDCl_3$) δ 8.87–8.80 (16H, m, H2, 3, 7, 8, 12, 13, 17, 18), 8.12 (12H, s, *ortho*), 8.08 (4H, d, *J* 9, H34), 8.02 (4H, d, *J* 9, H21), 7.78 (6H, s, *para*), 7.57 (4H, d, *J* 9, H35), 7.11 (4H, s, ND), 6.93 (4H, d, *J* 9, H22), 4.60 (4H, s, H46), 4.49 (2H, br, H23), 4.44 (4H, t, *J* 6, H26), 4.01 (4H, t, *J* 6, H33), 3.79 (4H, t, *J* 6, H27), 3.63 (4H, t, *J* 3, H30), 3.58 (4H, t, *J* 3, H31), 3.52 (8H, m, H28, 29), 3.44 (4H, t, *J* 6, H32), 1.53 (108H, s, *t-butyl*), −3.28 (4H, s, H25).

2,7-Bis(2-(2-(2-(2-(4-(phen-4-yl)methyl)carboxamido-propionyloxy)-ethoxy)-ethoxy)-ethoxy)-ethyl)benzo[*lmn*]-[3,8]phenanthroline-1,3,6,8-tetraone 15

This was synthesised by a similar procedure to that used for **2**, using the dicarboxylic acid thread (28 mg, 3.42×10^{-5} mol), EDC (16.3 mg, 8.55×10^{-5} mol), HOBT (18.5 mg, 1.37×10^{-4} mol), 4-toluidine (7.3 mg, 6.84×10^{-5} mol) and dry DCM (23 mL). The mixture was stirred at RT for 3 d. Purification was carried out on a preparative TLC silica plate using 5% MeOH–DCM as the eluant to obtain **15** as a yellow oil (8.5 mg, 25%); ^{1}H NMR (300 MHz, $CDCl_3$) δ 8.67 (4H, s, ND), 7.77 (2H, br, H23), 7.30 (4H, d, *J* 8, Hc), 6.98 (4H, d, *J* 8, Hb), 4.42 (4H, t, *J* 5, H26), 4.19 (4H, t, *J* 5, H33), 3.83 (4H, t, *J* 5, H27), 3.69–3.50 (20H, m, H28–32), 2.73 (4H, d, *J* 6, H35), 2.62 (4H, d, *J* 6, H34), 2.22 (6H, s, Ha).

2,7-Bis(2-(2-(2-(2-(4-(dinitrophen-2,4-yl)10,15,20-tris((3,5-di-*tert*-butyl)phenyl)porphyrinyl)carboxypropionyloxy)-ethoxy)-ethoxy)-ethoxy)-ethyl)benzo[*lmn*]-[3,8]phenanthroline-1,3,6,8-tetraone 16

To dicarboxylic acid thread unit (50 mg, 6.11×10^{-5} mol) and 2,4-dinitrophenol (22 mg, 12.20×10^{-5} mol) in 8 mL of dry DCM was added dicyclohexylcarbodiimide (DCC) (0.032 g, 15.28×10^{-5} mol) and the mixture was stirred overnight at RT (under N_2, dark). The crude mixture was then washed with ice cold water, partitioned with DCM and dried (Na_2SO_4). Excess solvent was removed *in vacuo.* The residue was dissolved in DCM and run through a short plug of silica using 10% MeOH–DCM as the eluant to isolate the by-product urea derivative. A final purification was carried out on a preparative TLC silica plate using 5% MeOH–DCM as the eluant to obtain **16** as a yellow oil (23.9 mg, 34%); ^{1}H NMR (300 MHz, $CDCl_3$) δ 8.92 (2H, s, Hx), 8.72 (4H, s, ND), 8.51 (2H, d, *J* 3, Hy), 7.54 (2H, d, *J* 9, Hz), 4.42 (4H, t, *J* 5, H26), 4.23 (4H, t, *J* 5, H33), 3.82 (4H, t, *J* 5, H27), 3.67–3.56 (20H, m, H28, 29, 30, 31, 32), 2.98 (4H, t, *J* 2, H35), 2.79 (4H, t, *J* 2, H34).

2,7-Bis(2-(2-(3-carboxypropionyloxy)-ethoxy)-ethyl)benzo[*lmn*]-[3,8]phenanthroline-1,3,6,8-tetraone 22

A mixture of 2,7-bis(2-(2-hydroxyethoxy)-ethyl)benzo[*lmn*]-[3,8]phenanthroline-1,3,6,8-tetraone (104 mg, 0.24 mmol), 4-(*N*,*N*-dimethylamino)pyridine DMAP (2.9 mg, 23.5 μmol, 10% mol), dry $CHCl_3$ (16 mL), Et_3N (70.8 mg), succinic anhydride (0.278 g, 2.8 mmol) and THF (3 mL) was stirred for 3 d. The solvent was removed *in vacuo*, the residue taken up in DCM, and washed with HCl (dil. aq), water, and dried (Na_2SO_4). Removal of excess solvent gave **21** as a pinkish yellow solid (150 mg, quantitative); mp 156–159 °C; *m/z* (ES-MS) ($C_{30}H_{30}N_2O_{14}$): [M + Na]$^+$ 665.161 (calcd. 665.159); ^{1}H NMR (300 MHz, $CDCl_3$) δ 8.76 (4H, s, ND), 4.48 (4H, t, *J* 5, H26), 4.18 (4H, t, *J* 6, H29), 3.89 (4H, t, *J* 5, H27), 3.72 (4H, t, *J* 4, H28), 2.30 (8H, s, H34, 35).

2,7-Bis(2-(2-(3,5-(phen-3-yl)10,15,20-tris((3,5-di-*tert*-butyl)phenyl)porphyrinyl)carboxypropionyloxy)-ethoxy)-ethyl)benzo[*lmn*]-[3,8]phenanthroline-1,3,6,8-tetraone 17 and 2-((2-(2-(3,5-(phen-3-yl)10,15,20-tris((3,5-di-*tert*-butyl)phenyl)porphyrinyl)carboxypropionyloxy))-7-[(2-(2-(3-carboxypropionyloxy)]-ethoxy)-ethyl)benzo[*lmn*]-[3,8]phenanthroline-1,3,6,8-tetraone 18

Synthesised as for **2**, using the dicarboxylic acid axle **22** (15 mg, 2.35×10^{-5} mol), freshly distilled $CHCl_3$ (12 mL), EtOH (15 μL), dry Et_3N (19.6 mg, 1.94×10^{-4}), EDC (39.6 mg, 2.07×10^{-4} mol), HOBT (13.0 mg, $0.96 \times 10^{--4}$ mol) and hydroxy phenyl porphyrin (50 mg, 5.16×10^{-5} mol). After 3 d (N_2, dark), excess EDC was added and the reaction was then stirred for a further 1 d. An initial purification was carried out on preparative TLC silica plates using 50% petroleum spirit–$CHCl_3$ as the eluant before a final purification was carried out (preparative TLC silica plates) using 30% petroleum spirit–$CHCl_3$ as the eluant to obtain the bis porphyrin stoppered adduct **17** and mono porphyrin stoppered adduct **18**.

17 as a purple solid (from MeOH–$CHCl_3$) (15.0 mg, 25%); mp 238–241 °C; *m/z* (ES-MS) ($C_{166}H_{182}N_{10}O_{14}$): [M + 2H]$^{2+}$ 1271.703 (calcd. 1271.699); ^{1}H NMR (300 MHz, $CDCl_3$) δ 8.84 (16H, m, H2, 3, 7, 8, 12, 13, 17, 18), 8.41 (6H, s, *ortho$_1$*) *and* (2H, peak hidden underneath, H21), 7.89 (6H, s, *ortho$_2$*), 7.89–7.85 (2H, d, H22), 7.79 (6H, m, *para*), 7.64 (2H, t, H23), 7.48 (2H, d, H24), 6.67 (4H, s, ND), 4.12 (4H, t, *J* 6, H26), 3.96 (4H, t, *J* 6, H29), 3.57 (4H, t, *J* 6, H27), 3.38 (4H, t, *J* 6, H28), 2.98 (4H, t, *J* 6, H35), 2.78 (4H, t, *J* 6, H34), 1.62 (54H, s, *t-butyl$_1$*), 1.47 (54H, s, *t-butyl$_2$*), −3.51 (4H, s, H25).

18 as a purple solid (from MeOH–$CHCl_3$) (29.0 mg, 75%); mp 136–141 °C; *m/z* (ES-MS) ($C_{100}H_{110}N_6O_{14}$): [M + Na]$^+$ 1641.801 (calcd. 1641.798), [M + H]$^+$ 1619.811 (calcd. 1619.816); ^{1}H NMR (300 MHz, $CDCl_3$) δ 8.84–8.82 (8H, m, H2, 3, 7, 8, 12, 13, 17, 18), 8.73–8.70 (3H, m, *ortho$_1$*), 7.80–7.78 (3H, m, *ortho$_2$*), 7.76–7.73 (3H, m, *para*), 7.71 (1H, s, H21), 7.64–7.58 (2H, m, H22, 23), 7.49 (1H, d, *J* 9, H24), 6.94 (2H, d, *J* 8, ND_2), 6.86 (2H, d, *J* 8, ND_2), 4.19 (2H, t, *J* 9, H26), 4.09–3.99 (8H, m, H29, 38, 41, 46), 3.60–3.56 (4H, m, H27, 40), 3.46 (2H, d, *J* 9, H39), 3.38 (2H, d, *J* 9, H28), 3.10 (2H, d, *J* 9, H35), 2.85 (2H, d, *J* 9, H34), 2.47 (4H, s, H36, 37), 1.74 (27H, s, *t-butyl$_1$*), 1.44 (27H, s, *t-butyl$_2$*), 1.20 (3H, *t*, *J* 6, H47), −4.13 (2H, s, H25).

Conclusions

Charge-transfer interactions resulting from π–π stacking of naphthodiimides with meso-substituted porphyrins are significant in both intra- and inter-molecular systems. In the absence of more strongly competitive influences, such as aromatic solvents or steric interference through either coordinated ligands in metalloporphyrins, or facially encumbered porphyrins, these interactions are maintained in solution, and are enhanced at lower temperatures. In flexibly linked porphyrin–naphthodiimide (POR–NDI–POR) systems, these interactions lead to distinct S-shaped foldamers, whereas more rigid systems exhibit intermolecular stacking, which is concentration and temperature dependent.

These interactions can be used to advantage in the design and construction of supramolecular systems containing these entities, either as a template motif in their assembly, or as a recognition element in the final system. They have considerable potential in supramolecular assemblies involving porphyrins, especially dynamic and controllable systems that utilise the rich photo- and electro-chemistry available in the diversity of metalloporphyrins. Neutral and charged systems incorporating rotaxanes, catenanes, nanotubes and helicates can be designed using this motif, in both thermodynamically- and kinetically-controlled self-assembly. For viable working devices, their attachment to surfaces and interfaces has already been demonstrated, and will no doubt be the subject of ongoing research.

Acknowledgements

This work was funded by a grant from the Australian Research Council.

Notes and References

1 S. J. Langford, M. J. Latter and C. P. Woodward, *Photochem. Photobiol.*, 2006, **82**, 1530–1540; S. V. Bhosale, C. H. Jani and S. J. Langford, *Chem. Soc. Rev.*, 2008, **37**, 331–342.
2 D. G. Hamilton, J. E. Davies, L. Prodi and J. K. M. Sanders, *Chem.–Eur. J.*, 1998, **4**, 608–620.
3 D. G. Hamilton, N. Feeder, S. J. Teat and J. K. M. Sanders, *New J. Chem.*, 1998, 1019–1021; Q. Zhang, D. G. Hamilton, N. Feeder, S. J. Teat, J. M. Goodman and J. K. M. Sanders, *New J. Chem.*, 1999, **23**, 897–903; Y. Nakamura, S. Minami, K. Iizuka and J. Nishimura, *Angew. Chem., Int. Ed.*, 2003, **42**, 3158–3162; G. D. Fallon, M. A. P. Lee, S. J. Langford and P. J. Nichols, *Org. Lett.*, 2004, **6**, 655–658.
4 J. G. Hansen, N. Feeder, D. G. Hamilton, M. J. Gunter, J. Becher and J. K. M. Sanders, *Org. Lett.*, 2000, **2**, 449–452.
5 T. Iijima, S. A. Vignon, H. R. Tseng, T. Jarrosson, J. K. M. Sanders, F. Marchioni, M. Venturi, E. Apostoli, V. Balzani and J. F. Stoddart, *Chem.–Eur. J.*, 2004, **10**, 6375–6392; S. A. Vignon, T. Jarrosson, T. Iijima, H. R. Tseng, J. K. M. Sanders and J. F. Stoddart, *J. Am. Chem. Soc.*, 2004, **126**, 9884–9885.
6 G. Kaiser, T. Jarrosson, S. Otto, Y. F. Ng, A. D. Bond and J. K. M. Sanders, *Angew. Chem., Int. Ed.*, 2004, **43**, 1959–1962.
7 S. I. Pascu, C. Naumann, G. Kaiser, A. D. Bond, J. K. M. Sanders and T. Jarrosson, *Dalton Trans.*, 2007, 3874–3884.
8 G. D. Pantos, P. Pengo and J. K. M. Sanders, *Angew. Chem., Int. Ed.*, 2007, **46**, 194–197; G. D. Pantos, J.-L. Wietor and J. K. M. Sanders, *Angew. Chem., Int. Ed.*, 2007, **46**, 2238–2240.
9 M. A. Houghton, A. Bilyk, M. M. Harding, P. Turner and T. W. Hambley, *J. Chem. Soc., Dalton Trans.*, 1997, 2725–2733; A. C. Try, M. M. Harding, D. G. Hamilton and J. K. M. Sanders, *Chem. Commun.*, 1998, 723–724.
10 R. J. Abraham, F. Eivazi, H. Pearson and K. M. Smith, *J. Chem. Soc., Chem. Commun.*, 1976, 698–699; R. J. Abraham, F. Eivazi, H. Pearson and K. M. Smith, *J. Chem. Soc., Chem. Commun.*, 1976, 699–701; A. E. Alexander, *J. Chem. Soc.*, 1937, 1813–1816; C. A. Hunter and J. K. M. Sanders, *J. Am. Chem. Soc.*, 1990, **112**, 5525–5534; C. A. Hunter, *Chem. Soc. Rev.*, 1994, 101–109; D. Mauzerall, *Biochemistry*, 1965, **4**, 1801–1810.
11 C. A. Hunter, M. N. Meah and J. K. M. Sanders, *J. Chem. Soc., Chem. Commun.*, 1988, 692–694; C. Roger, M. G. Muller, M. Lysetska, Y. Miloslavina, A. R. Holzwarth and F. Wurthner, *J. Am. Chem. Soc.*, 2006, **128**, 6542–6543.
12 H. L. Anderson, C. A. Hunter and J. K. M. Sanders, *J. Chem. Soc., J. Chem. Soc., Chem. Commun.*, 1989, 226–227; C. A. Hunter, J. K. M. Sanders, G. S. Beddard and S. Evans, *J. Chem. Soc., Chem. Commun.*, 1989, 1765–1767; J. L. Sessler, C. T. Brown, D. O'Connor, S. L. Springs, R. Wang, M. Sathiosatham and T. Hirose, *J. Org. Chem.*, 1998, **63**, 7370–7374; A. Osuka, R. Yoneshima, H. Shiratori, T. Okada, S. Taniguchi and N. Mataga, *Chem. Commun.*, 1998, 1567–1568; K. P. Ghiggino, J. A. Hutchison, S. J. Langford, M. J. Latter, M. A.-P. Lee and M. Takezaki, *Aust. J. Chem.*, 2006, **59**, 179–185; K. Saito, Y. Kashiwagi, K. Ohkubo and S. Fukuzumi, *J. Porphyrins Phthalocyanines*, 2006, **12**, 1371–1379.
13 M. J. Gunter, N. Bampos, K. D. Johnstone and J. K. M. Sanders, *New J. Chem.*, 2001, **25**, 166–173; M. J. Gunter, *Eur. J. Org. Chem.*, 2004, 1655–1673.
14 M. J. Gunter and S. M. Farquhar, *Org. Biomol. Chem.*, 2003, **1**, 3450–3457.
15 M. J. Gunter and Z. Merican, *Supramol. Chem.*, 2005, **17**, 521–528.
16 K. D. Johnstone, K. Yamaguchi and M. J. Gunter, *Org. Biomol. Chem.*, 2005, **3**, 3008–3017.
17 H. Shiratori, T. Ohno, K. Nozaki, I. Yamazaki, Y. Nishimura and A. Osuka, *J. Org. Chem.*, 2000, **65**, 8747–8757; D. Gosztola, M. P. Niemczyk and M. R. Wasielewski, *J. Am. Chem. Soc.*, 1998, **120**, 5118–5119; K. Okamoto, Y. Mori, H. Yamada, H. Imahori and S. Fukuzumi, *Chem.–Eur. J.*, 2004, **10**, 474–483.
18 K. D. Johnstone, N. Bampos, J. K. M. Sanders and M. J. Gunter, *New J. Chem.*, 2006, **30**, 861–867; K. D. Johnstone, N. Bampos, J. K. M. Sanders and M. J. Gunter, *Chem. Commun.*, 2003, 1396–1397; K. M. Mullen, K. D. Johnstone, M. Webb, N. Bampos, J. K. M. Sanders and M. J. Gunter, *Org. Biomol. Chem.*, 2008, **6**, 278–286.
19 D. J. Hill, M. J. Mio, R. B. Prince, T. S. Hughes and J. S. Moore, *Chem. Rev.*, 2001, **101**, 3893–4012; S. H. Gellman, *Acc. Chem. Res.*, 1998, **31**, 173–180.
20 M. T. Stone and J. S. Moore, *Org. Lett.*, 2004, **6**, 469–472; W. Zhang, D. Horoszewski, J. Decatur and C. Nuckolls, *J. Am. Chem. Soc.*, 2003, **125**, 4870–4873; A. P. Bisson, F. J. Carver, D. S. Eggleston, R. C. Haltiwanger, C. A. Hunter, D. L. Livingstone, J. F. McCabe, C. Rotger and A. E. Rowan, *J. Am. Chem. Soc.*, 2000, **122**, 8856–8868.
21 S. Ghosh and S. Ramakrishnan, *Angew. Chem., Int. Ed.*, 2005, **44**, 5441–5447; Q. Z. Zhou, X. K. Jiang, X. B. Shao, G. J. Chen, M. X. Jia and Z. T. Li, *Org. Lett.*, 2003, **5**, 1955–1958.
22 G. J. Gabriel, S. Sorey and B. L. Iverson, *J. Am. Chem. Soc.*, 2005, **127**, 2637–2640; J. J. Reczek and B. L. Iverson, *Macromolecules*, 2006, **39**, 5601–5603.
23 M. Tabata and J. Nishimoto, in *The Porphyrin Handbook*, ed. K. M. Kadish, K. M. Smith and R. Guilard, Academic Press, San Diego, 2000, vol. 9, pp. 387–391.
24 M. J. Blanco, J. C. Chambron, V. Heitz and J. P. Sauvage, *Org. Lett.*, 2000, **2**, 3051–3054.
25 C. L. Barney, E. W. Huber and J. R. McCarthy, *Tetrahedron Lett.*, 1990, **31**, 5547–5550.